Available online at www.sciencedirect.com

SCIENCE DIRECT

Cellular Signalling 17 (2005) 1111–1124

CELLULAR SIGNALLING

www.elsevier.com/locate/cellsig

Early immune response and regulation of IL-2 receptor subunits

Millie Hughes-Fulford[a,b,c,*], Eiko Sugano[a,b], Thomas Schopper[d], Chai-Fei Li[a,b], J.B. Boonyaratanakornkit[a,e], Augusto Cogoli[d]

[a]*Northern California Institute for Research and Education, San Francisco, CA, United States*
[b]*Laboratory of Cell Growth, San Francisco, CA, United States*
[c]*University of California San Francisco and Veteran's Affairs Medical Center, San Francisco, CA, United States*
[d]*Space Biology, ETH Zürich, Switzerland*
[e]*UC Berkeley, Berkeley, CA, United States*

Received 6 February 2004; received in revised form 29 September 2004; accepted 11 December 2004
Available online 25 February 2005

Abstract

Affymetrix oligonucleotide arrays were used to monitor expression of 8796 genes and probe sets in activated T-cells; analysis revealed that 217 genes were significantly upregulated within 4 h. Induced genes included transcription factors, cytokines and their receptor genes. Analysis by semi-quantitative RT-PCR confirmed the significant induction of IL-2, IL-2Rγ and IL-2Rα. Forty-eight of the 217 induced genes are known to or predicted to be regulated by a CRE promoter/enhancer. We found that T-cell activation caused a significant increase in CREB phosphorylation furthermore, inhibition of the PKC pathway by GF109203 reduced CREB activation by 50% and inhibition of the PKA pathway caused a total block of CREB phosphorylation and significantly reduced IFNγ, IL-2 and IL-2Rα gene expression by approximately 40% ($p<0.001$). PKCθ plays a major role in T-cell activation: inhibition of PKC significantly reduced the expression of IFNγ, IL-2 and IL-2Rα. Since PKC blocked activation of CREB, we studied potential cross-talk between the PKC and the PKA/MAPK pathways, PMA-stimulated Jurkat cells were studied with specific signal pathway inhibitors. Extracellular signal-regulated kinase-2 (ERK2) pathway was found to be significantly activated greater than seven-fold within 30 min; however, there was little activation of ERK-1 and no activation of JNK or p38 MAPK. Inhibition of the PKA pathway, but not the PKC pathway, resulted in inhibition of ERK1/2 activation at all time points, inhibition of MEK1 and 2 significantly blocked expression of IL-2 and IL-2Rα. Gene expression of IL-2Rα and IFNγ was dependent on PKA in S49 wt cells but not in kin$^-$ mutants. Using gel shift analysis, we found that forskolin activation of T-cells resulted in activation of AP1 sites; this increase in nuclear extract AP1 was significantly blocked by MEK1 inhibitor U0126. Taken together, these results suggest that the PKA in addition to PKC and MAPK pathways plays a role in early T-cell activation and induction of IL-2, IL-2Rα and IFNγ gene expression.
Published by Elsevier Inc.

Keywords: T-cell activation; Immune response; Protein kinase A; Interleukin-2; IL-2 receptor; IL-2 receptor subunits

1. Introduction

Activation of naïve/resting T-cells is initiated by the binding of a foreign antigen presented by an MHC class I or class II molecule on an antigen-presenting cell (APC) to the T-cell receptor. A second signal delivered by the same APC is required for full activation, with CD28 being the primary co-stimulatory molecule. The expression of interleukin-2 (IL-2) induces synthesis of interleukin-2 receptor (IL-2R); both are essential for efficient immune response, T-cell proliferation and progression from the G0 to G1 phase [1–6].

In vitro, the first signal delivered by the antigen can be mimicked by the use of agents such as PMA (phorbol 12-myristate 13-acetate) and calcium ionophores, or by anti-CD3 antibodies and lectins. Binding of concanavalin A (con A), a plant lectin, causes the activation of protein tyrosine

* Corresponding author. Laboratory of Cell Growth, University of California, Department of Medicine, and Veteran's Affairs Medical Center, 4150 Clement Street MC151F, San Francisco, CA 94121, United States. Tel.: +1 415 221 4810x2749; fax: +1 415 750 6667.
E-mail address: milliehf@aol.com (M. Hughes-Fulford).

0898-6568/$ - see front matter. Published by Elsevier Inc.
doi:10.1016/j.cellsig.2004.12.016

kinases and subsequent phospholipase C (PLC) activation. PLC cleaves phosphoinositol diphosphate (PIP_2) into diacylglycerol (DAG) and inositol triphosphate (IP_3). DAG activates PKC, with IP_3 causing an increase in intracellular calcium concentration [7].

Previous studies have shown that T-cell activation is dependent on the duration of a mitogenic stimulus and on mitogen concentration [6,8]. T-lymphocytes exposed to con A or other mitogens for at least 2 h will transcribe and secrete IL-2. PKC activation as well as cytosolic calcium upregulation are known to contribute to the induction of transcription factors including *c-fos*, *c*-jun, NFAT (nuclear factor of activated T-cells), *c-myc* or NF-κB (nuclear factor κB) within 30 min of activation. The protein expression of these immediate-early genes in turn activates IL-2 and IL-2R expression [5,9]. The IL-2 receptor has three subunits: α, β and γ. The primary function of the α subunit is to bind IL-2; when alone, it binds IL-2 with low affinity [10,11]. However, together with the β and γ subunits, it forms the high affinity IL-2R and all three subtypes are essential for proliferative signaling [1].

This study examines gene expression and synthesis of IL-2 receptor subunits as well as IL-2 and IFNγ at early time points following activation. We show that expression of IL-2Rα and γ subunits as well as IL-2 and IFNγ are significantly upregulated within 4 h after con A/anti-CD28 stimulation. Of the genes significantly induced, 22% had either potential or known promoter units regulated by CRE. Activation of T-cells caused a greater than 100-fold increase in pCREB, which was blocked by PKA inhibitor H-89. Activated T-cells had increased activation of ERK2, which was inhibited with PKC or PKA inhibitors. Activation of T-cells with PMA caused a similar induction of IL-2Rα, which was inhibited by specific inhibitors of the PKA, PKC or MAPK pathways. In addition, analysis of gene expression in wt and kin^- S49 T-cells show a dependence on PKA for expression of IL-2Rα and IFNγ. Studies of T-cell signal transduction pathways demonstrated that ERK2 was phosphorylated within minutes of activation, while P38, JNK and PI3K remained unchanged. These results suggest that T-cell activation, which is dependent on IL-2Rα, IL-2 and IFNγ expression, is mediated via MAPK, PKC and in part by transient PKA signaling during early stages of activation.

2. Methods

2.1. Materials

S49 wild type and kin^- cells, Jurkat E6-1 cells, antibiotic, horse sera, HEPES buffer and DME-21 (DMEM supplemented with 4 mM L-glutamine, 25 mM glucose and 3.7 g/L sodium bicarbonate) were obtained from the University of California Cell Culture Facility (San Francisco, CA). Guanidinium thiocyanate was from Fisher Scientific (Springfield, NJ). Sodium citrate was from Acros Organics (Geel, Belgium). Isopropanol, phenol/chloroform/isoamyl alcohol (125:24:1), sodium acetate, concanavalin A (con A), protein G, PMA, A23187, TriReagent and chloroform were obtained from Sigma (St. Louis, MO). Anti-CD28 was from BD PharMingen (San Diego, CA). Ficoll-Hypaque was from Biochrom KG (Berlin, Germany). The human recombinant IL-2, human T-cell enrichment columns and quantikine immunoassay kits were obtained from R&D Systems (Minneapolis, MN). β-2-Mercaptoethanol was from Fluka (Buchs, Switzerland). Oligonucleotides were synthesized by Operon Technologies (Alameda, CA). Forskolin, PKA inhibitor H-89 and PKC inhibitor GF109203X were obtained from Biomol (Plymouth Meeting, PA). MEK1 inhibitor U0126 was obtained from Calbiochem (La Jolla, CA). Polyacryl carrier was obtained from Molecular Research Center (Cincinnati, OH). 100-bp DNA marker was from Life Technologies (Rockville, MD). All RT-PCR reagents were from Applied Biosystems (Foster City, CA), and reverse transcription and subsequent amplification were carried out on the Robocycler 40 from Stratagene (San Diego, CA). Phosphorylated p38 MAP kinase (Thr180/Tyr182), p38 MAP kinase, phosphorylated JNK/SAPK (Thr183/Tyr185) phospho-p42/44 (phosphoThr202/ phosphoTyr204) MAP kinase (ERK) and p42/44 MAP (ERK) kinase antibodies were purchased from Cell Signaling Technologies (Beverly, MA). Phosphorylated PI3 kinase (Tyr-508) antibody was purchased from Santa Cruz Biotechnology (Santa Cruz, CA). Phosphorylated PKA (Ser96) and phosphorylated CREB (Ser133) antibodies were purchased from Upstate (Charlottesville, VA). The goat–anti-rabbit horseradish peroxidase conjugated secondary antibodies were purchased from Jackson Immunoresearch (Bar Harbor, ME). Supersignal pico enhanced chemiluminescence kits were purchased from Pierce (Rockford, IL). CyQuant™ Kit was purchased from Molecular Probes (Eugene, OR). All other reagents were from Sigma-Aldrich (St. Louis, MO). Electrophoretic-mobility shift assay (EMSA) gel-shift assay for AP-1 transcription factor was purchased from Panomics Inc. (Redwood City, CA).

2.2. Isolation and activation of human lymphocytes

Cell preparation and stimulation procedures were performed by the Space Biology Group at ETH Zürich in Switzerland or by the Laboratory of Cell Growth at San Francisco. PBL were separated from a buffy coat obtained from the blood bank of the Red Cross (Zurich) or Stanford Blood Center (Palo Alto, CA) by Ficoll-Hypaque density gradient centrifugation. Subsequent T-lymphocyte purification was performed using human T-cell enrichment columns, which isolated $CD3^+$ T-cells via high affinity negative selection. Lymphocytes were maintained at room temperature overnight in RPMI 1640 containing 10 mg/ml gentamycin, 2 mg/ml sodium bicarbonate and supplemented with 10% FCS, until activation the following day. Cells were aliquoted into 2 ml Eppendorf tubes to a final

concentration of 2×10^6 cells/ml. T-lymphocytes were activated with 5–10 μg/ml con A, 4 μg/ml anti-CD28 and 2 μg/ml protein G. Activated samples were incubated at 37 °C for 2, 4 or 24 h. Control samples were unstimulated. For the experiments in which the inhibitors were used, inhibitor was added to the activator solution. GF109203X was added at 0.25 μM and H-89 was added at 30 μM concentration, the manufacturer's recommended concentration. All samples were centrifuged at 13,000×*g* for 45–60 s after incubation. Supernatant was removed and 1 ml of 4 M guanidinium thiocyanate (GITC) in 750 mM sodium citrate buffer, pH 7 with *N*-laurylsarcosine and β-2-mercaptoethanol was added to each in order to lyse the cells and stabilize the RNA. After vigorous vortexing, all sample lysates and supernatants were placed in −80 °C until shipment to VAMC, San Francisco, for analysis.

2.3. Cell culture

S49 wild type and kin$^-$ cells were grown in DME-21 supplemented with 10% heat inactivated horse serum, antibiotic and 10 mM HEPES. Cells were plated at 6.7×10^5 cells/ml in 6-well plates and serum deprived in 4% heat inactivated horse serum for 16 h before being treated with or without 10 μM forskolin, 30 μM H-89 or both for 4 h. Jurkat E6-1 cells were grown in RPMI-1640 supplemented with 10% FCS, antibiotic, L-glutamine, 12.5 mM HEPES, sodium pyruvate and non-essential amino acids. Cells were seeded at 350,000 cells/ml in 6-well plates and serum deprived in 2% FCS for 18 h before being treated with 50 ng/ml PMA and 500 ng/ml A23187 with or without 10 U IL-2 and with or without 1 μM or 10 μM H-89 or 10 μM U0126 for 24 h. Cells were treated with inhibitors 1 h prior to stimulation.

2.4. PCR primers

Novel gene-specific RT-PCR primers (see Table 1) for human IL-2, IL-2Rα, IL-2Rβ, IL-2Rγ and IFNγ and mouse IL-2, IL-2Rα and IFNγ were designed by this lab and were synthesized by Operon Technologies. Primer pairs spanned at least one intron of each gene and were selected according to optimal priming features-minimal primer dimer formation, no hairpin loops, optimal internal stability (stable 5′ termini), PCR product between 200 and 600 base pairs, 20–23 mer primer length and close annealing temperatures of the upper and lower primers. The RT-PCR linear range was determined using increasing cycle numbers.

2.5. Semi-quantitative RT-PCR validation of microarray data

Linear semi-quantitative RT-PCR was performed for analysis of gene expression and was carried out as described previously [12,13]. To verify the reliability and robustness of data obtained from microarray analysis, RT-PCR was performed on our five genes of interest that are key in early immune response. Gene specific primers for 18S (Ambion) and IL-2, IL-2Rα, IL-2Rβ, IL-2Rγ and IFNγ were designed by our lab and synthesized by Operon. Band intensity from cDNA product from the three donors, each with four independent biological samples was determined using the

Table 1
Primers used in RT-PCR

Gene	Orientation	Sequence (5′→3′)	Product size (bp)	T_m (°C)	Cycle #	Based on Genbank accession ID
18S	Sense	TCAAGAACGAAAGTCGGAGG	488	63	24	Ambion, Inc. (Austin, TX)
	Anti-sense	GGACATCTAAGGGCATCACA				
Human sequences						
IL-2	Sense	TACAAGAATCCCAAACTCACCAG	470	53	32	S77834
	Anti-sense	GGCACAAAAAGAATCATAAAAGA				
IL-2Rα	Sense	ATCCCACACGCCACATTCAAAGC	347	58	30	NM_000417
	Anti-sense	TGCCCCACCACGAAATGATAAAT				
IL-2Rβ	Sense	GCCCCCATCTCCCTCCAAGT	529	66	29	NM_000878
	Anti-sense	AGGGGAAGGGCGAAGAGAGC				
IL-2Rγ	Sense	GGAAGCCGTGGTTATCTCTGTT	407	58	26	L19546
	Anti-sense	GGTGGGTTGAATGAAGGAAAGT				
IFNγ	Sense	TTGGGTTCTCTTGGCTGTTACTG	426	53	26	X13274
	Anti-sense	CATCTGACTCCTTTTTCGCTTCC				
Murine sequences						
IL-2	Sense	CTCTACAGCGGAAGCACAG	417	54	various	X01772
	Anti-sense	GGGCTTGTTGAGATGATGC				
IL-2Rα	Sense	GTTGCTGATGTTGGGGTTTC	306	54	26	NM_008367
	Anti-sense	TGCATGTCTGTTGTGGTTTG				
IFNγ	Sense	CAGGCCATCAGCAACAACAT	496	54	26	M28621
	Anti-sense	CAACCCCGCAATCACAGTCT				

SigmaGel software (Sigma), and gene expression was represented as amount of RT-PCR product normalized to 18S product.

2.6. RNA extraction and cleanup for microarrays and semi-quantitative RT-PCR

After thawing and adding 2 M sodium acetate with phenol/chloroform/isoamyl alcohol (125:24:1), the lysates were spun at 12,000×*g* in 4 °C for phase separation of RNA. Total RNA was precipitated overnight in isopropanol with polyacryl carrier, washed with 75% ethanol and resuspended in DEPC water. RNA from the S49 and Jurkat E6-1 cells were isolated using the TriReagent® protocol as recommended by Sigma. RNA concentration and purity was determined by measuring absorbance at 260 nm and 280 nm with a GeneQuant (Pharmacia) or a Bioanalyzer (Agilent). 0.3 μg total RNA was run on a denaturing formaldehyde gel (1% agarose) or 100 ng total RNA was loaded on the Bioanalyzer to verify RNA integrity and to check for degradation.

2.7. Microarray sample preparation

The following protocol was modified from the Affymetrix GeneChip® Expression Analysis Technical Manual: 1.8 μg of total RNA at a minimum concentration of 0.18 μg/μL was aliquoted for first strand and second strand cDNA synthesis using a HPLC purified oligo-(dT) primer (Affymetrix) and 200 U SuperScript II RT (Invitrogen). All incubations were performed in a thermocycler. 10 μL of the eluted cDNA was then aliquoted for in vitro transcription, amplification and biotin labeling following the protocol provided for the BioArray High Yield™ RNA Transcription Labeling Kit (Enzo). The reaction mixture was incubated for 10 h at 37 °C. A typical yield of approximately 40 μg cRNA was attained after transcription. The cRNA was then fragmented using a 5× fragmentation buffer with magnesium cations (Affymetrix), and electrophoresis was used to ensure that the RNA was sufficiently fragmented. 10 μg of the labeled cRNA was hybridized at a final concentration of 0.05 μg/μL onto Human Focus Arrays (Affymetrix), each with 8796 probe sets, at 45 °C for 16 h. The arrays were washed and stained using the Fluidics Station 400, scanned using a GeneArray Scanner and image analysis was performed using Affymetrix Microarray Suite 5.0 (MAS).

2.8. Data analysis

After background subtraction and image processing in MAS, data normalization was performed in GeneSpring™ 6.0 to reduce technical variability during sample preparation. The distribution of gene expression for each chip was normalized to its corresponding median, because cRNA concentration used for array hybridization was identical across samples. The global normalization method was chosen for the one-color Affymetrix technology, since the resulting gene expression histograms for the samples were similar and centered at one.

Differential gene expression during activation was identified through applying three stringent filters. First, only genes flagged in MAS with a present call in at least one sample, indicating a large difference in signals between perfect match and mismatch probe pairs, were considered for subsequent analysis. Next, a two-fold change cutoff on the normalized signals and a parametric paired *t*-test with $p<0.05$ was used as a statistical filter on the logarithm of the normalized data from the three biological donors. Several consensus sequences were searched against the UCSC genome database http://genome.ucsc.edu (April 2003).

2.9. ELISA

Cell culture supernatant from T-lymphocytes activated in the presence of inhibitors were analyzed for the presence of IL-2, IL-2sRα and IFNγ. Protocols recommended by the ELISA manufacturer were followed. For the IL-2 sRα ELISA, analysis was made on data in which samples were diluted 1:2 instead of 1:10 since the concentration of protein was too low with the latter dilution. A Dynatech MR5000 microplate reader (Dynatech Laboratories, Chantilly, VA) was used to take readings at 450 nm with wavelength correction at 570 nm. Data were analyzed using the BioLinx 2.0 software (Dynatech).

2.10. Statistical analysis

T-lymphocyte data were derived from independent triplicate or quadruplicate samples for each incubation period on each of three separate subjects. Data on the S49 and Jurkat E6-1 cells were also derived from three independent samples. For each time point or treatment condition, mean and S.D. were calculated and are shown on figures. ANOVA was performed using GraphPad InStat version 3.01 for Windows 95/NT and Bonferroni post test (GraphPad Software, San Diego, CA) to obtain *p* values.

2.11. Promoter sequence analysis

MacDNASIS™ software (Hitachi, San Bruno, CA) was used to analyze the 5′ flanking promoter regions of desired genes. Sequences were obtained from Genbank and the positions of functional regulatory elements were obtained from the literature.

2.12. Immunoblot analysis

Cells were activated for times described, and lysed in the lysis buffer previously described [14]. 0.25 μM of GF109203X or 15 μM of U0126 were added 1 h prior

to activation. Equal amounts of protein were loaded and transferred to a nitrocellulose membrane (Amersham, Piscataway, NJ). Membranes were probed with phosphorylated p38 MAP kinase (Thr180/Tyr 182), p38 MAP kinase, phosphorylated JNK/SAPK (Thr183/Tyr185), phospho-p42/44 (phospho-Thr202/ phospho-Tyr204) MAP kinase (ERK), p42/44 MAP (ERK) kinase phosphorylated PI-3 kinase (Tyr-508), phosphorylated PKA (Ser 96) or phosphorylated CREB (Ser133) antibodies. Identification of ERK-1 and ERK2 was made by comparison to known standards. Proteins were detected by enhanced chemiluminescence (Supersignal Pico kit) and exposed on autoradiography film. Films were scanned and bands quantified by the UNSCANIT™ gel Automated Digitizing Systems 5.1 (Silk Scientific, Orem, Utah).

2.13. Electrophoretic-mobility shift assay (EMSA) gel-shift assay for AP1

Human T-lymphocytes were isolated and activated with 10 μM of forskolin for 1 h, one set of three independent samples was pre-incubated with 10 μM of U0126 1 h prior to activation. Using the EMSA kit from Panomics, nuclear protein was isolated by methods established by Feramisco et al. [15]. 5 μg of nuclear extract from each independent sample (n=3) was screened for AP-1 binding according to manufacturer's protocol (www.panomics.com). Gel shifts were detected using a specific biotinylated AP1 probe and then were imaged using enhanced chemiluminescence (Supersignal Pico kit) and exposed on autoradiography film. Films were scanned and shifted bands were quantified by the UNSCANIT™ gel Automated Digitizing Systems 5.1 (Silk Scientific, Orem, Utah).

3. Results

3.1. T-cell activation affects global gene expression distribution

T-cells were isolated from three human donors and activated with con A and anti-CD28 for 4 h. Total RNA from unactivated T-cells (0 h) and activated T-cells was extracted, amplified and fragmented, cRNA was hybridized to human focus arrays. Signal intensities for each gene were normalized to show differential gene expression during T-cell activation (Fig. 1). Points above the top diagonal are genes upregulated above two-fold, the central diagonal has slope=1, while points below the bottom diagonal include genes downregulated above two-fold during activation. The points in Fig. 1 are centered around the central diagonal with several outliers beyond the two-fold lines. The 217 blue data points represent genes that were significantly upregulated by activation. These were selected by applying three stringent filters: two-fold change from unactivated, a present call filter and a significance filter (Table 2). Forty-eight of the 217 genes are known experimentally to be regulated by a CRE enhancer or their promoter region contained the CRE consensus sequence TGANNTCA within 1000 nucleotides upstream of the transcription start site. Among the most interesting and most strongly stimulated genes are those of the IL-2 family and its receptor subunits.

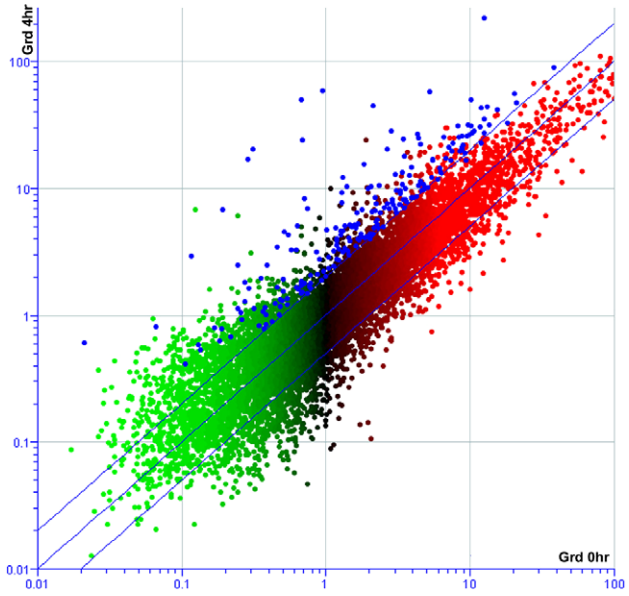

Fig. 1. Plots of normalized signal for 8796 probe sets from the average of 6 chips from 3 donors show disparate changes in gene expression during activation. All genes are plotted in this graph. The abscissa contains data from the activated T-cells at 4 h; the ordinate contains the data from the unactivated T-cells. Blue data points represent the genes that are significantly upregulated two or more fold over controls.

3.2. RT-PCR validation of microarray analysis for IFNγ, IL-2, IL-2Rα, IL-2Rβ and IL-2Rγ

The expression profiles for the cytokines IFNγ, IL-2 and the receptors IL-2Rα, IL-2Rβ and IL-2Rγ generated from microarray analysis and linear RT-PCR are similar. The normalized signals from microarray analysis for combined donors are seen in Table 2, while normalized band intensities from RT-PCR are seen in Fig. 2. Standard error bars are derived from four independent biological samples and ** indicates $p<0.001$ from a Student's t-test with respect to 0 h. Significant upregulation of IFNγ, IL-2 and IL-2Rα was observed during T-cell activation by 4 h. The normalized signal for IL-2Rβ and IL-2Rγ remained relatively static after the initial stimulation for all three donors. On resting T-cells, β and γ chains are expressed constitutively and bind IL-2 with moderate affinity. However, upon activation, T-cells begin synthesis of the α chain to form a high-affinity heterotrimeric receptor to trigger growth, proliferation and differentiation.

Table 2
Upregulated genes predicted or known by experiment to be transcriptionally regulated by a CRE promoter

	Ratio (4/0 h)	Accession no.
Apoptosis induction		
B-cell CLL/lymphoma 10 (BCL10)	3.3	AF082283
β-Amyloid binding protein precursor (BBP)	2.8	AA012917
Apoptosis inhibition		
BCL2-related protein A1 (BCL2A1)	9.3	NM_004049
TNF receptor-associated factor 1 (TRAF)	5.7	NM_005658
Biosynthesis and transport		
Solute carrier family 7 member 5 (SLC7A5)	3.7	AB018009
Cytochrome P450, 51 (CYP51)	3.6	NM_000786
Ornithine decarboxylase I (ODC)	3.0	NM_002539
JTV1	2.5	NM_006303
Seryl-tRNA synthetase (SARS)	2.5	NM_006513
Catabolism		
Superoxide dismutase 2, mitochondrial (SOD2)	3.1	X15132
Hexokinase (HK2)	2.5	AI761561
Cell cycle regulation or DNA replication		
Retinoic acid induced 2 (RAI2)	4.2	NM_021785
Cell structure, nuclear and cytoskeletal maintenance		
Dynactin 4 (DCTN4)	2.5	NM_016221
Cell surface proteins involved in cell adhesion		
Extracellular matrix protein 2 (ECM2)	4.6	NM_001393
CD97	3.0	NM_001784
Cytokines, chemokines, growth factors and secreted products		
Lymphotoxin α (TNF super family, member 1) (LTA)	66.9	NM_000595
Interleukin 2 (IL2)	55.9	NM_000586
Chemokine ligand 1 (XCL1)	25.5	NM_002995
Tumor necrosis factor (TNF superfamily, member 2) (TNF)	21.4	NM_000594
Chemokine ligand 4 (CCL4)	17.8	NM_002984
Chemokine ligand 3 (CCL3)	6.3	NM_002983
Tumor necrosis factor super family, member 14 (TNFSF14)	6.1	NM_003807
Mannan-binding lectin serine protease 1 (MASP1)	4.7	NM_001879
Interleukin 6 (IL6)	2.9	NM_000600
Macrophage migration inhibitory factor (glycosylation-inhibiting factor) (MIF)	2.8	NM_002415
Cytokine, chemokine and growth factor receptors		
Interleukin 2 receptor, alpha (IL2RA)	9.0	K03122
Tumor necrosis factor receptor superfamily, member 9	7.4	NM_001561
Interleukin 2 receptor, gamma (SCID) (IL2RG)	2.8	NM_000206
Cytokine, chemokine and growth factor receptors		
Tumor necrosis factor receptor superfamily, member 6 (TNFRSF6)	2.1	AA164751
Immediate early response genes		
Phorbol-12-myristate-13-acetate-induced protein 1 (PMAIP1)	9.5	NM_021127
Early growth response 2 (Krox-20 homolog, Drosophila) (EGR2)	8.0	NM_000399
Early growth response 1 (EGR1)	5.1	NM_001964
Activating transcription factor 3 (ATF3)	3.9	NM_001674
Signal transduction		
Dual specificity phosphatase 5 (DUSP5)	10.1	U16996
Non-metastatic cells 2 (NME2)	5.2	NM_000269
Serum/glucocorticoid regulated kinase (SGK)	3.9	NM_005627
Non-metastatic cells1 (NME1)	3.1	NM_002512
Transcription		
v-maf musculoaponeurotic fibrosarcoma oncogene homolog F (avian) (MAFF)	11.7	AL021977
STAT1	7.7	NM_007315
Interferon regulatory factor 4 (IRF4)	5.8	D78261
Nuclear receptor subfamily 4, group A, member 2 (NR4A2)	5.3	S77154
Aryl hydrocarbon receptor (AHR)	2.9	NM_001621
v-rel reticuloendotheliosis viral oncogene homolog B, NFkB3 (RELB)	2.5	NM_006509
cAMP responsive element binding protein 1 (CREB1)	2.2	AI655737
Structure specific recognition protein 1 (SSRP1)	2.2	NM_003146
RNA processing and turnover		
ATP-binding cassette, subfamily E, member 1 (ABCE1)	2.6	AI002002
ATP/GTP-binding protein (HEAB)	2.3	NM_006831
ELAVL1 (Hu antigen R)	2.0	BC003376

Genes involved in T-cell activation after 4 h that are potentially or known to be regulated by a CRE enhancer are upregulated during activation. Data was normalized globally to the median expression of each chip and to the corresponding genes in the 0 h baseline experiment for the three donors. Ratios show relative abundance of gene expression in activated T-cells over non-activated. Genes reported are significantly (p<at least 0.05) upregulated at least two-fold by activation as detected by Affymetrix™ gene chip and GeneSpring 6™ analysis. Text in italics are genes that are known experimentally to be upregulated by CRE element; others had the TGANNTCA consensus sequence for the CREB/ATF in their promoter region.

3.3. Time course of gene induction on con A/anti-CD28-activated purified T-lymphocytes

A previous study observed IL-2 and IL-2R mRNA expression between 0 and 12 h following activation and

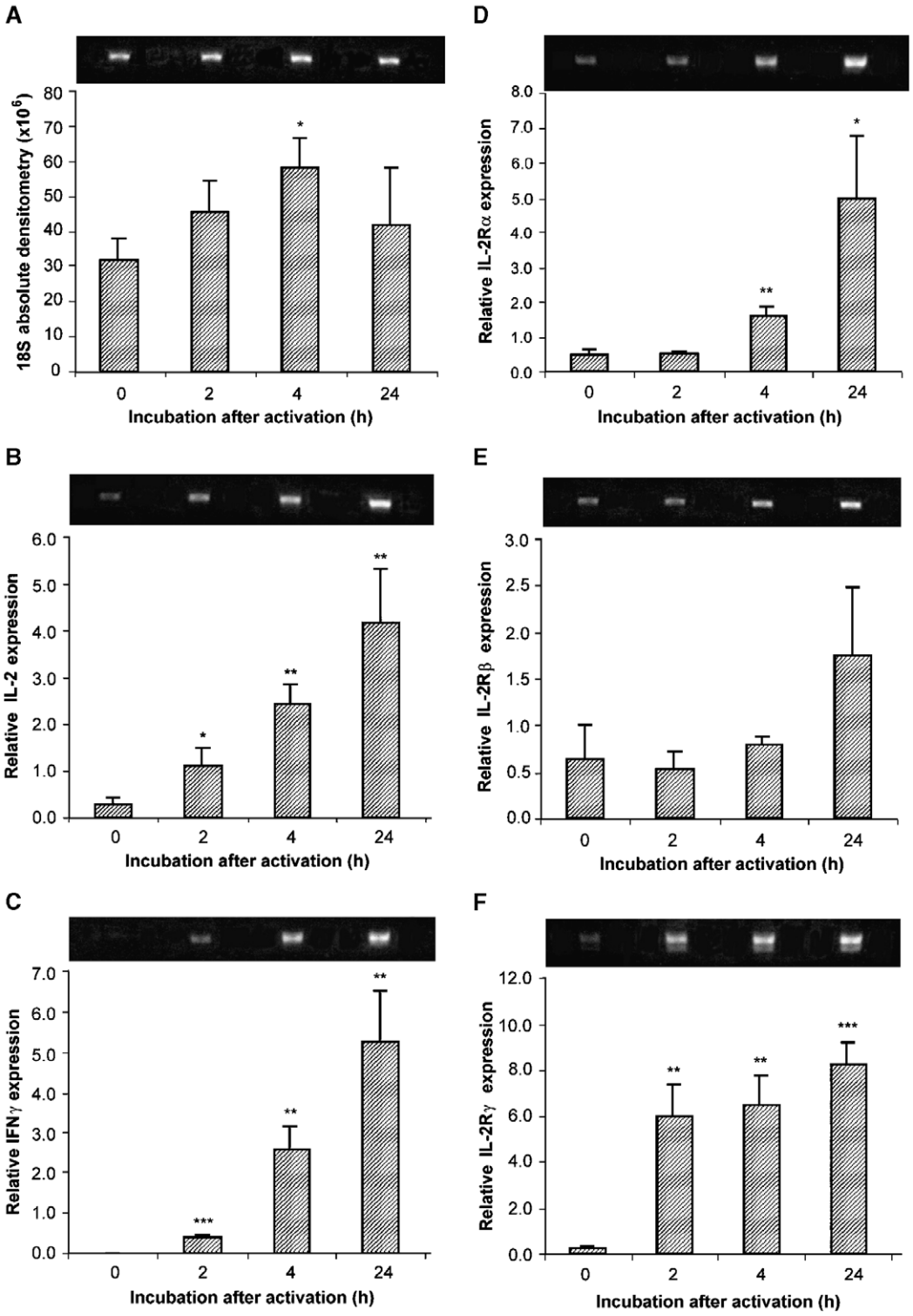

Fig. 2. Induction of gene expression in con A/anti-CD28/protein G-activated T-lymphocytes at t=0, 2, 4 and 24 h. T-lymphocytes activated for the indicated time points, RNA isolated and subsequent RT-PCR performed. mRNA expression levels were measured relative to 18S. All mRNA levels were normalized to 18S product. Statistical significance was determined using Student's unpaired t-test. Bars represent means±S.D. of independent triplicate samples from one donor, *p<0.05, **p<0.01, ***p<0.001.

found that both were downregulated in the RPM, however, the studies were done on one sample and did not have statistical significance [16]. In the current study, early induction of gene expression was studied on con A activated cells incubated for 0, 2 and 4 h, and resultant RNA was analyzed by linear RT-PCR and Affymetrix oligonucleotide arrays at 4 h. Resting T-lymphocytes expressed low basal levels of IL-2Rα, IL-2Rβ and IL-2Rγ as well as IL-2 and

IFNγ mRNA (Fig. 2). Significant induction of IL-2 and IFNγ mRNA occurred by 2 h, and expression was further induced at 4 and 24 h (Fig. 2B,C). Two hours after stimulation, IL-2Rγ mRNA expression was significantly upregulated and remained induced for the remaining 22 h (Fig. 2F). IL-2Rα mRNA expression was significantly upregulated at 4 h and was further induced at 24 h (Fig. 2D). IL-2Rβ was constitutive throughout the 24-h period with no statistical differences between the time points (Fig. 2E). Although relative levels of gene expression can vary from donor to donor, the pattern of induction showed in Fig. 2 is representative of the three donors.

3.4. Con A-induced IL-2 and IL-2R mRNA expression is dependent on both the PKA and PKC signaling pathways

In order to identify potential signaling pathways through which con A and anti-CD28 induces gene expression, we analyzed the effect of specific PKA and PKC inhibitors. 0.25 μM of the PKC inhibitor GF109203X significantly downregulated IFNγ, IL-2 and IL-2Rα mRNA expression 1.8-, 1.7- and 1.4-fold, respectively (Table 3). IL-2Rβ and γ expressions were neither suppressed nor induced with PKC inhibitor. Although 30–100 μM H-89 is routinely used for inhibition of PKA, treatment with as little as 15 μM significantly downregulated IFNγ mRNA expression four-fold. IL-2 and IL-2Rα mRNA expression were also significantly downregulated 4- and 14-fold, respectively. No significant change was observed in the expression of IL-2Rβ and IL-2Rγ.

3.5. IL-2 cytokine production is downregulated by inhibitor of PKA

Interleukin-2 and IFNγ are produced and released upon T-cell activation; IL-2 production is required for T-cell proliferation and differentiation upon activation. Since relative levels of IFNγ, IL-2 and IL-2Rα mRNA were significantly downregulated by PKA and PKC inhibitors, we analyzed protein expression using ELISA on the culture medium from the RNA samples. IL-2 protein synthesis was significantly depressed three-fold upon treatment with 30 μM H-89 (Table 4). No significant effect of either 25 μM or 0.5 μM GF109203X was noted on the production of IL-2. No significant changes of IFNγ or IL-2Rα in the culture medium were shown between the control samples and samples treated with either one of the inhibitors.

Table 4
Protein expression of T-lymphocytes upon con A activation with PKA or PKC inhibitor

Activation[a]	Concentration (pg/ml)		
	IFNγ	IL-2	IL-2Rα
Control	12.4±2.1	5.4±1.1	4.4±1.5
H-89			
+15 μM	3.7[b]	1.7±1.3*	6.5±1.9
+30 μM	9.2±3.8	1.7±0.6**	6.0±1.6
GF109203X			
+0.25 μM	8.6±1.9	2.4±1.8	7.8±3.0
+0.50 μM	13.4±10.6	4.2±1.6	8.2±5.3

[a] Media taken for ELISA taken from experiment, in Fig. 2.
[b] Means without SD, represented two independent sample, the concentration of the third sample was too low to detect.
* $p<0.05$.
** $p<0.01$.

3.6. Kin⁻ mutant cells show regulation of IL-2Rα and IFNγ mRNA expression by cAMP

To further examine the role of the PKA pathway in T-cell activation, we stimulated S49 wild type and kin⁻ cells with

Table 3
Gene expression of T-lymphocytes upon con A activation with PKA or PKC inhibitor

Treatment[a]	mRNA expression[b]					
	18S	IFNγ	IL-2	IL-2Rα	IL-2Rβ	IL-2Rγ
H-89						
Control	23.07±0.19	2.14±0.38	3.48±0.17	3.27±0.36	1.99±0.23	2.85±0.30
+15 μM	25.52±9.93	0.39±0.46**	2.10±0.43**	0.94±0.65**	1.58±0.16	2.26±0.76
+30 μM	23.35±6.06	0.12±0.07***	0.83±0.50***	0.22±0.04***	0.71[c]	2.88±1.06
GF109203X						
Control	32.05±0.53	2.08±0.28	1.96±0.23	1.86±0.08	1.26±0.13	1.33±0.04
+0.25 μM	40.95±36.83***	1.18±0.06**	1.19±0.02**	1.33±0.19*	1.13±0.37	1.33±0.10
+0.50 μM[c]	36.83	1.17	1.12	0.97	1.10	1.67

[a] T-lymphocytes were activated with 5 μg/ml of con A alone or with PKA inhibitor, H-89 or PKC inhibitor, GF109203X, for 4 h as described in Methods.
[b] mRNA expression levels are reported as the mean±S.D. of triplicate samples and are relative to 18S. The mean values of 18S mRNA expression represent absolute levels divided by 10^6.
[c] Values without S.D.s represent means of two samples.
* $p<0.05$.
** $p<0.01$.
*** $p<0.001$.

forskolin, a stimulator of adenylate cyclase [17] with or without PKA inhibitor H-89. S49 cells are mouse T-lymphoma cells derived from the BALB/c strain [18]. The S49 kin$^-$ cells lack functional PKA activity due to a gene mutation in its regulatory subunit, preventing cAMP from binding to the enzyme [19].

S49 wt and kin$^-$ cells grown in 4% horse sera lacked IFNγ mRNA expression. However, addition of 10 μM forskolin for 4 h induced IFNγ mRNA expression in wild type but not kin$^-$ cells (Fig. 3), further implicating the dependency of early T-cell activation on the PKA pathway. PKA inhibitor, H-89, caused a near complete inhibition of IFNγ mRNA expression in wt cells, showing that forskolin induced expression of IFNγ through the cAMP-dependent PKA pathway.

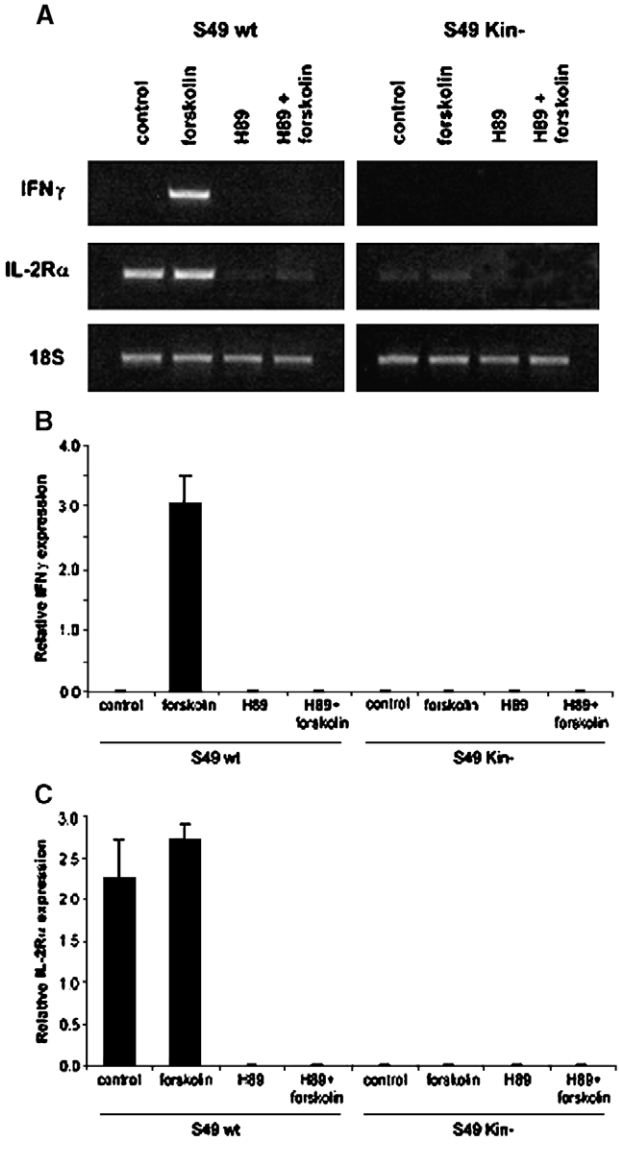

Fig. 3. Downregulation of IFNγ and IL-2Rα mRNA expression in S49 kin$^-$ cells. Cells were treated with forskolin, H-89 or both for 4 h and then analyzed for gene expression. (A) RT-PCR product bands for IFNγ, IL-2Rα and 18S; each band is representative of a triplicate. (B) IFNγ and (C) IL-2Rα gene expression relative to 18S. Bars represent means±S.D. of independent triplicate samples for each treatment.

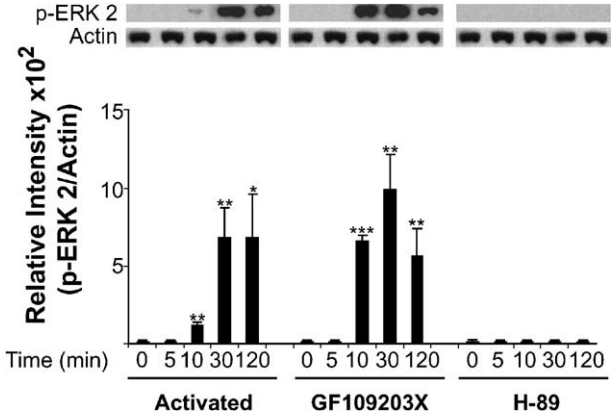

Fig. 4. Induction of phosphorylated ERK protein (p-ERK) inhibited by PKA inhibitor H-89. To investigate the induction of p-ERK, all buffy-coat isolated peripheral T-cells were activated with 4 μg/ml anti-CD28 and 5 μg/ml con A for 30 min. For inhibition of pathways, 0.25 μM of GF109203X (GF) and 15 μM of H-89 was added 1 h prior to activation in samples. Total protein was harvested at 0, 5, 10, 30 and 120 min after activation. Western blot was performed using 20 μg of protein against p-ERK (Thr202/Tyr204) polyclonal antibody (Cell Signal, MA). Bars represent mean±S.D. of intensity of bands (n=3) corrected to internal standard Actin. *p<0.05, **p<0.01, ***p<0.0001 with Student's t-test.

IL-2Rα mRNA was expressed in unstimulated and forskolin-stimulated samples of S49 wild type cells, but H-89 completely inhibited this expression, showing that even in slowly growing cells, IL-2Rα expression is regulated by PKA. In the S49 kin$^-$ cells, IL-2Rα expression was too low a copy number to measure. Due to low message expression of IL-2 in the S49 cell type, as previously reported [20], dependency of its expression on the PKA pathway could not be shown using these cells.

3.7. MAPK activation plays a significant role in early immune response

To determine if T-cell activation was mediated through a MAPK pathway and to confirm the action of the inhibitors, we examined ERK 1/2 phosphorylation as a marker of MAPK kinase activation. Thirty minutes after con A/anti-CD28 activation, samples were collected for Western blot analysis. Using an anti-phospho-ERK 1/2 antibody, we observed that early in activation there was a significant phosphorylation of primarily, ERK2 (Fig. 4). No phosphorylation of either ERK isoform was detectable in the non-activated controls, indicating there is negligible ERK activity in quiescent cells. Furthermore, activation did not induce phosphorylation of JNK or p38MAPK. When activated cells were pre-treated with PKA inhibitor H-89, phosphorylation of ERK2 was totally blocked and there was no effect of PKC inhibitor GF109203X on ERK2 phosphorylation.

3.8. PKA and MAPK pathway inhibitors inhibit PMA induction of cytokines and receptors

Induction of expression of IFNγ, IL-2 and IL-2Rα by PMA was abolished by U0126 as seen in Table 5. Since IL-2 secretion and binding of the cytokine to its receptor induces T-cell proliferation and IL-2R expression, we examined the effect of exogenous IL-2 on Jurkat E6-1 cells pretreated with specific PKA or MAPK inhibitors and stimulated with PMA and calcium ionophore, A23187. We used MEK inhibitor U0126, since it has been shown to selectively inhibit ERK activation, leaving the JNK and p38 pathways unaffected [21]. Stimulation of cells with PMA/A23187 or PMA/A23187/L-2 significantly upregulated IFNγ, IL-2 and IL-2Rα gene and protein expression (Fig. 5, Table 4). Both the specific MEK inhibitor U0126 and PKA inhibitor H-89 significantly inhibited key gene and protein expression. Addition of human recombinant IL-2 did not cause a significant upregulation of IFNγ or IL-2Rα expression in any of the PMA-stimulated samples that were pretreated with inhibitor. A significant upregulation ($p<0.05$) with the addition of exogenous IL-2 was only seen in the IL-2 gene expression of PMA-stimulated samples (Fig. 5).

3.9. MEK inhibitor of ERK1/2 phosphorylation causes significant decrease in expression of IL-2R subunits

As seen in Table 5, the specific ERK1/2 inhibitor U0126 inhibited PMA mediated IL-2 and IL-2Rα gene expression by at least 65%. The specific ERK1/2 inhibitor U0126 inhibited IFNγ, IL-2 and IL-2Rα protein synthesis by 96%, 99% and 94%, respectively (Fig. 5). There was no significant change in the synthesis of total ERK during the same time period.

3.9.1. Increase in AP1 factors in activated T-cells

As seen in Fig. 6, there was little AP1 found in the nuclear extract of the non-activated T-cells. A significant increase in AP1 was seen with forskolin activation of human T-cells. This increase in AP1 transcription factor with forskolin activation was significantly inhibited with

Table 5
Protein expression of PMA-stimulated Jurkat E6-1 cells treated with PKA or MAPK inhibitor and exogenous IL-2[a]

Treatment group		Concentration (pg/ml)		
		IFNγ	IL-2	IL-2Rα
1	Control	0.6±0.5	<0.01	<0.01
2	PMA	32.4±3.1	1166.4±56.7	147.2±13.5
3	PMA+IL-2	29.8±1.8	>2000[c]	165.8±10.6
4	30 μM H-89	<0.01	0.4	<0.01
5	30 μM H-89+PMA	<0.01	0.9±0.5***	<0.01
6	30 μM H-89+PMA+IL-2	1.3±1.1	>2000	<0.01
7	10 μM U0126+PMA	1.4±0.8***	12.7±4.7***	8.4
8	10 μM U0126+PMA+IL-2	1.7	>2000[c]	2.2

[a] Treatment groups 3, 5, 7 and 9 were compared to treatment group 2 for statistical significance using Student's unpaired *t*-test.
*** $p<0.001$.

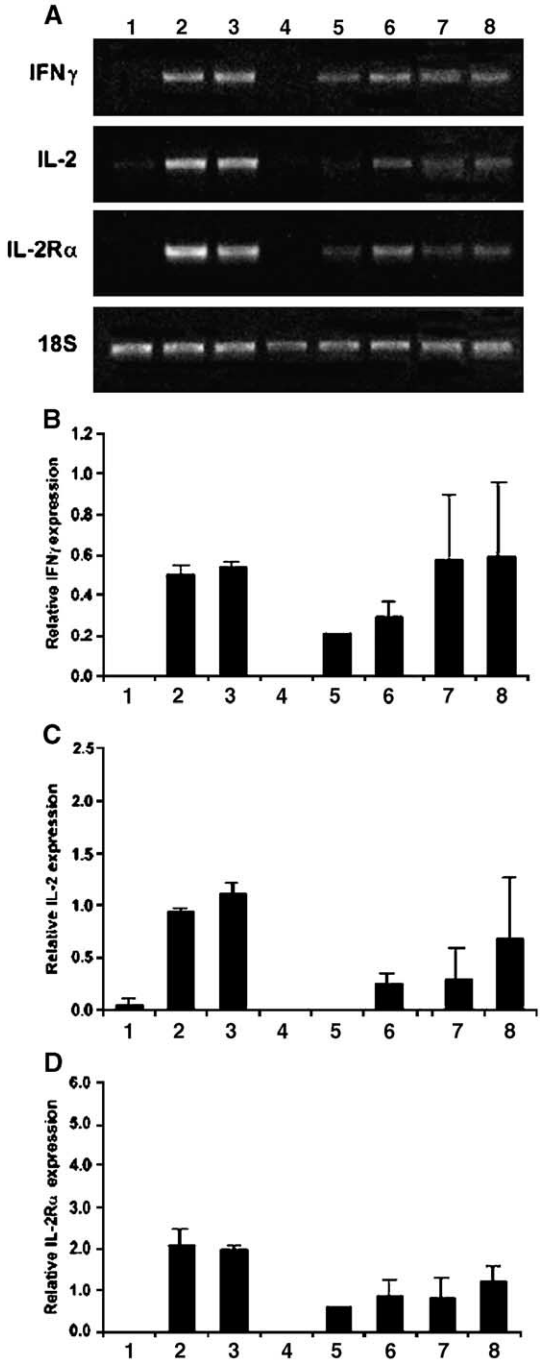

Fig. 5. Effect of exogenous IL-2 on Jurkat E6-1 cells pretreated with PKA or MEK inhibitor. Cells were pretreated for 1 h with 1 or 30 μM H-89 or 10 μM U0126 and stimulated with PMA/A23187 with or without IL-2. Lane 1, control; lane 2, *PMA*/A23187; lane 3, PMA/A23187+IL-2; lane 4, 30 μM H-89; lane 5, 30 μM H-89+PMA/A23187; lane 6, 30 μM H-89+PMA/A23187+IL-2; lane 7, 10 μM U0126+PMA/A23187; lane 8, 10 μM U0126+PMA/A23187+IL-2 (A) RT-PCR product bands for IFNγ, IL-2, IL-2Rα and 18S; each band is representative of a triplicate. (B) IFNγ, (C) IL-2, (D) IL-2Rα gene expression relative to 18S. Bars represent means±S.D. of independent triplicate samples for each treatment.

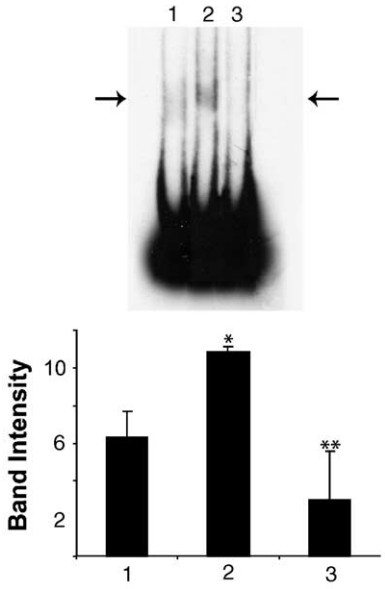

Fig. 6. Transcriptional factor AP1 is activated by forskolin and MEK1 inhibitor U0126 inhibits AP1. To investigate activation of AP1, nuclear extract of peripheral T-cells was extracted 1 h after activation by 10 μM of forskolin and 10 μM of U0126 was added to a portion of the cells 1 h prior to activation. Gel shift against AP1 was performed using 5 μg of nuclei extract according to the manufacturer's protocol. One representative sample is shown from each treatment: (1) non-activated samples, (2) samples activated with 10 μM forskolin and (3) samples activated with 10 μM forskolin pretreated with U0126. There was no significant difference in the unactivated controls and U0126 treated activated cells. Bars represent mean±S.D. of intensity of bands (n=3). *p<0.05 compares activated cells (2) to non-activated samples (1); **p<0.05 compares U0126 treated activated cells (3) to activated cells (2) with Student's t-test.

pre-incubation with U0126 MEK inhibitor. Each group had four independent samples (n=4).

3.9.2. Increase in CREB phosphorylation with activation

The activation of CREB by phosphorylation was increased in con A/anti-CD28 activated T-cells with little or no pCREB found in the non-activated samples. When cells were pre-treated with PKC specific inhibitor GF109203X, activation of CREB was reduced by approximately 50% and was completely blocked by PKA inhibitor H-89. Each group had four independent samples.

4. Discussion

The immune response is initiated by con A activation of the T-cell receptor (TCR) complex and co-stimulation by anti-CD28, which causes resting T-cells to exit G0 and enter G1 of the cell cycle. It is IL-2 and IL-2R that drive the progression past the G1 checkpoint thus enabling proliferation to occur [1]. The details of the signal transduction pathways leading from early TCR and CD28 activation to expression of Il-2, IFNγ, IL-2R subunits are not fully understood.

Examination of global gene expression in activated T-cells showed a significant upregulation of 217 genes by at least 2-fold. Of these, approximately twenty-five percent are regulated by a CRE, suggesting that transcriptional activation by the CREB/ATF leucine zipper family is significantly upregulated during early T-cell activation. In addition to the 28 genes known experimentally to be regulated by a CRE enhancer, the CRE consensus sequence TGANNTCA was identified within 1000 nucleotides upstream of the transcription start site in 20 other genes that passed three filters [2-fold change on ground, present call filter and a significance filter] (Table 2). These 48 genes include 5 genes encoding tumor necrosis factors or their receptors that are involved in proliferation. In addition, retinoic acid induced 2, an activator of the STAT1 promoter, is involved in cell cycle regulation and growth. An increase in gene expression of cell surface proteins, including CD97, a G-protein coupled receptor that is an indicator of T-cell activation, was observed within 4 h of activation. Three chemokines XCL1, CCL3 and CCL4 also were characterized by significant upregulation during activation. XCL1 interacts with a G-protein coupled receptor to regulate T-cell migration and is stimulated by CD28 engagement. CCL3 and CCL4 encode homologous chemokines involved in inflammation and cell entry from a G0 to a G1 phase in the cell cycle and are linked within the genome by <14 kb. NME1 and NME2 are similarly separated by only 18 kb and encode proteins that heterodimerize to act as a G-protein associated kinase. RelB contains two upstream CRE sequences and encodes a transcription factor that interacts with NFκB. These potentially co-regulated genes are involved in pathways responsible for normal T-cell activation. The 48 genes, predicted or functionally regulated by the CREB/ATF family of transcription factors, were all significantly upregulated during activation. It is known that early activation of T-cells includes a transient rise in cAMP within the first 5 min, returning to normal within 2 h [22–24]. Using inhibitors of specific pathways at early timepoints, this transient rise in cAMP has been shown to regulate another cytokine, IL-13 [22]. Similar results with IL-2 and IL-2R are seen in Table 3. Early activation of T-cells results in CREB phosphorylation, this activation was inhibited by PKC inhibitor and completely blocked by PKA specific inhibitor H-89 (Fig. 7). These data suggest possible cross-talk between PKA and PKC, such interactions between the PKC and PKA pathways has been previously described [25–29] are in support of our findings.

The role of the PKCθ in T-cell activation has been well established [30], while the role of the PKA pathway during early activation has not been fully explored. Since con A activates phospholipase C via G_α protein and leads to the activation of PKC, it was expected that PKC dependent genes would be suppressed with the addition of a specific PKC inhibitor. Significant downregulation of

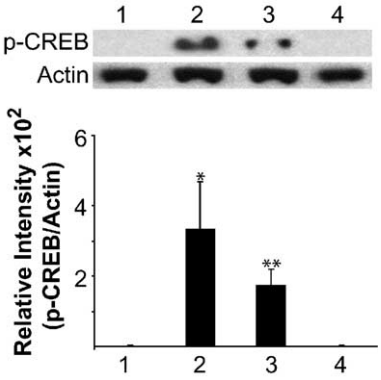

Fig. 7. Induction of phosphorylation of CREB protein (p-CREB) is partially inhibited by PKC inhibitor GF109203X and totally inhibited by PKA inhibitor H-89. To investigate the induction of p-CREB during activation, buffy-coat isolated peripheral T-cells were activated and treated with specific pathway inhibitors. Non-activated samples (lane 1) remained inactivated. Lane 2 has samples from T-cells activated with 4 μg/ml anti-CD28 and 5 μg/ml concanavalin A (con A) for 30 min (lane 3) T-cells activated and treated with 0.25 μM of GF109203X (GF) or (lane 4) T-cells activated and treated with 15 μM of H-89. 30 min after activation, total protein was harvested. Western blot was performed using 20 μg of protein against p-CREB (Ser 133) polyclonal antibody. One representative sample is shown for each treatment. Bars represent mean±S.D. of intensity of bands (n=3) corrected to internal standard Actin. *p<0.05, **p<0.01 with Student's t-test.

IL-2Rα, IL-2 and IFNγ gene expression was seen with 0.25 μM PKC inhibitor after incubation for 4 h (Table 3).

The gene induction of IFNγ, IL-2 and its receptor subunits are also consistent with predictions based on inspection of their respective promoter regions. Of the α, β and γ subunits, only the α subunit contains an IL-2 response element approximately −3780 relative to the transcription start position containing three sites, two of which bind STAT dimers [31,32]. In purified T-cells, IL-2 upregulation precedes IL-2Rα induction (Fig. 2). The γ subunit was induced within 2 h after activation, whereas expression of the β subunit showed no correlation of regulation relative to IL-2 transcript levels. Data from experiments using the specific PKA inhibitor H-89 show a loss of IL-2Rα, IL-2 and IFNγ gene induction. Of particular interest was the significant downregulation of IL-2 gene and protein expression levels, since IL-2 is a principal indicator of T-cell activation and is thought to be primarily regulated through a PKC pathway (Fig. 5, Tables 4 and 5). In comparison to the PKC inhibitor, the suppressive effect of the PKA inhibitor on these genes was at a greater magnitude with a near total loss of IL-2Rα and IFNγ gene induction. No significant change in the soluble form of IL-2Rα was detected in the culture medium, most likely a result of the brief 4-h incubation, a time period that would not show a significant change in protein synthesis. Protein concentrations of IFNγ in samples treated with H-89 were below the sensitivity threshold of the assay and were too low to detect in the culture medium.

In light of the above data, we were interested in determining whether the simultaneous stimulation of TCR/CD28 activates the MAPK pathway in T-lymphocytes in a MEK-dependent fashion and whether this pathway contributes to initiation of induction of the IL-2R genes and associated cytokines. We present data showing that ERK2 is activated within 10 min of T-cell stimulation by con A/anti-CD28 (Fig. 4) followed by a significant induction of IL-2 by 2 h and of IL-2Rα and interferon by 4 h. No phosphorylation of p38 or JNK was observed.

Several lines of evidence suggest that ERK may be involved in inducing the transcriptional activation of AP-1 response elements in TCR-responsive genes. ERK can upregulate c-Fos expression by phosphorylation of Elk-1, which binds the *c-fos* promoter. Both c-Fos and c-Jun bind to the AP-1 sites and contribute to the expression of the IL-2, IL-2Rα and IFNγ genes, suggesting that ERK2 may play a role in their transcriptional activation. Blocking the MAPK pathway with U0126 caused inhibition of T-cell ERK2 phosphorylation and subsequent inhibition of gene expression and protein synthesis of IL-2, IL-2Rα, IL-2Rγ and IFNγ. Although CD28 has been implicated in p38 MAPK activation, activation of this MAPK was not seen at early timepoints of this study. Blocking PKA activity with H-89 also inhibits expression of IL-2, IL-2Rα, IL-2Rγ and IFNγ. One of the first intracellular signals accompanying the antigen receptor stimulation is a transient increase in intracellular cAMP [23,24,33,34]. Recent reports have validated a role for cAMP and PKA in early signal transduction of T-cell regulation of interleukin 13 production [22]. PKA is also known to activate MAPK pathway in many cells and can be the primary target of hormonal stimulation for initiation of proliferation [35]. We report that blocking the PKC pathway does not inhibit pERK activation; however, when we block the PKA pathway, we completely block ERK phosphorylation during T-cell activation (Fig. 4). We significantly blocked the induction of IL-2Rα, IL-2 and IFNγ gene expression by at least 65% and IL-2Rα, IL-2 and IFNγ protein synthesis by 94% or more by blocking the PKA pathway during T-cell activation. The system is very sensitive to inhibition of PKA; even use of a sub-optimal dose of 1 μM H-89 caused a 36%, 39% or a 22% reduction of expression of IFNγ, IL-2 and IL-2Rα, respectively (data not shown). Furthermore, we analyzed the increase in pCREB 30 min after activation with con A and anti-CD28 and found an increase in pCREB of more than 100-fold in activated T-cells, this activation was decreased by approximately 50% with PKC inhibitor GF109203X and completely abolished with PKA inhibitor H-89.

Since there were no published reports of PKCθ activating the ERK 1/2 pathway, we examined the possibility that other pathways were involved in the early initiation of T-cell activation. Using Jurkat E6-1 cells, we show that the induction of IFNγ, IL-2 and IL-2Rα expression is dependent on the MAPK pathway, in addition to the PKA pathway (Fig. 3, Table 4). Our data is consistent with DeSilva et al.

who showed that MEK inhibitor U0126 decreases IL-2 mRNA levels [21]. Addition of exogenous IL-2 alone was insufficient to restore gene expression inhibited by PKA or MAPK inhibitor. When T-cells are activated by PMA, IFNγ, IL-2 and IL-2Rα were significantly up-regulated, however, inhibitors of the MAPK or PKA pathways were able to significantly block the induction (Fig. 5). These results further suggest that multiple signaling pathways are involved in the induction of genes necessary for T-cell proliferation.

Several reports have shown that constant pharmacological elevation of cAMP to superphysiological levels can inhibit T-cell activation. Ramstad et al. have reported that pretreatment of Jurkat T-cells with pharmaceutical levels (150 μM) of exogenous 8-CPT-cAMP and stimulated with anti-CD3 caused a PKA mediated inhibition of the Ras/MAPK pathway, downstream of PKC, via phosphorylation of Raf-1 [36]. However, our studies examine the relatively small and transient physiological rises of cAMP on early cell signaling. Experiments using normal and mutant S49 T-cells give further proof of the role of PKA in the induction pathway of genes is crucial in T-cell activation. Treatment of S49 wild-type cells with H-89 alone significantly inhibited IL-2Rα levels ($p<0.001$), and the presence of IL-2Rα in the unstimulated S49 wt cells demonstrated probable PKA involvement of IL-2Rγ expression during growth (Fig. 3). Furthermore, IFNγ gene expression, which was induced in forskolin-stimulated wt cells, was absent in kin$^-$ cells, supporting the role of a PKA-dependent pathway for IFNγ expression. We further examined the effect of forskolin activation in the T-cell and found a significant increase in nuclear AP1, which was downregulated by approximately 50% by MEK inhibitor U0126.

In conclusion, analysis of induction of over 8500 genes during early T-cell activation demonstrated an upregulation of 48 genes that had CRE/ATF motif, especially cytokines and their receptors, were among the most highly induced. We have illustrated key pathways that most likely are utilized during early activation. The pathway analysis is based on the work of others as well as our own. The activation of NFkB, CREB, ELK and AP-1 share subsets of the same upstream kinases to cross-talk with one another to achieve gene induction in the nucleus [25,27,28,37,38]. The signal pathways of PKC, ERK1 and ERK2 are common to the four transcription factors identified [39–45] and the regulation of the IL-2Rα subunit and cytokines IFNγ and IL-2 that are necessary for T-lymphocyte activation and proliferation that are activated by at least three of the four transcription factors. Examination of early activation events shows that critical

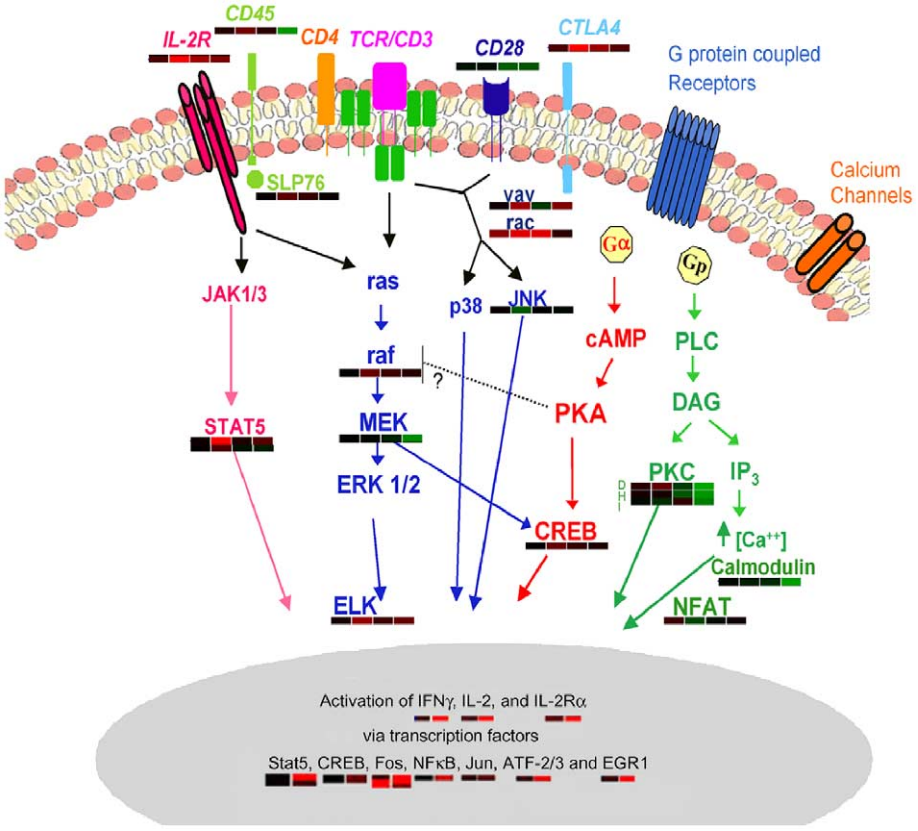

Fig. 8. Signaling pathway for T-cell activation notated with average gene expression at key points in the pathway: a unique shape and color as illustrated represent each transcription factor. Bold lines indicate regions of positive or negative regulation. Gene expression profiles are shown in order from unstimulated to stimulated (4 h) T-cells with red indicating upregulation and green indicating downregulation.

genes are induced as early as 2 h after T-cell activation. In early induction of T-cell gene expression, we have found that expression of IFNγ, IL-2 and IL-2Rα are dependent on PKC and PKA signal transduction and that pCREB and AP1 are significantly increased during activation (Figs. 6 and 7). Moreover, analysis of IL-2 protein expression demonstrates that inhibition of PKA activity significantly decreases IL-2 production within 4 h of activation. The importance of PKA in early T-cell activation is further demonstrated by use of S49 T-cell wt and kin^- mutants where IFNγ is induced by forskolin in the wild type cells with no effect on the gene expression in the kin^- T-cells. Moreover , inhibition of PKA activity in wt cells results in a significant inhibition of expression of IFNγ and IL-2Rα, suggesting a dependence on PKA signaling in early T-cell activation. PKA and MAPK inhibitors blocked PMA activation of Jurkat cells suggesting cross-talk between PKA and PKC signaling. Looking for upstream signal transduction, we found that ERK2 was phosphorylated within minutes of activation and inhibition of MAPK activity or PKA blocked activation of T-cells. Taken together, these data suggest that ERK2 plays a role in early T-cell activation of IL-2 and IL-2R subunits, most likely through both the PKC and PKA signaling pathways (Fig. 8).

Acknowledgements

We dedicate this paper to the families of the STS-107 crew that trained to conduct the Leukin experiment. This work was supported by collaboration between NASA and the PRODEX program of the European Space Agency. The NASA portion was supported by grant NAG-2-1286 in the Laboratory of Cell Growth, NCIRE, and a Department of Veteran's Affairs Merit Review, VAMC, San Francisco. The ESA portion was supported by Contract 13634/NL/VJ (IC) to ETH Zürich, Switzerland. Scientific heading: Immunobiology. Microarray hybridization support was provided by the General Clinical Research Center Core Genomics Laboratory operating under grant number M01RR00083-41 at San Francisco General Hospital.

References

[1] B.H. Nelson, D.M. Willerford, Adv. Immunol. 70 (1998) 1.
[2] A. Cogoli, J. Leukoc. Biol. 54 (3) (1993) 259.
[3] G.N. Gaulton, P. Williamson, Chem. Immunol. 59 (1994) 91.
[4] G.R. Crabtree, N.A. Clipstone, Annu. Rev. Biochem. 63 (1994) 1045.
[5] G.R. Crabtree, Science 243 (4889) (1989) 355.
[6] J.F. Modiano, J. Mayor, C. Ball, C.G. Chitko-McKown, N. Sakata, J. Domenico-Hahn, J.J. Lucas, E.W. Gelfand, Cell. Immunol. 197 (1) (1999) 19.
[7] M.J. Berridge, Crit. Rev. Immunol. 17 (2) (1997) 155.
[8] A. Weiss, R. Shields, M. Newton, B. Manger, J. Imboden, J. Immunol. 138 (7) (1987) 2169.
[9] V.C. Foletta, D.H. Segal, D.R. Cohen, J. Leukoc. Biol. 63 (2) (1998) 139.
[10] Y.W. He, T.R. Malek, Crit. Rev. Immunol. 18 (6) (1998) 503.
[11] Y. Minami, T. Kono, T. Miyazaki, T. Taniguchi, Annu. Rev. Immunol. 11 (1993) 245.
[12] J. Fitzgerald, T.J. Dietz, M. Hughes-Fulford, Endocrinology 141 (1) (2000) 291.
[13] M. Hughes-Fulford, V. Gilbertson, FASEB J. 13 (1999) S121, (Suppl.).
[14] J.P. Hatton, F. Gaubert, M.L. Lewis, Y. Darsel, P. Ohlmann, J.P. Cazenave, D. Schmitt, FASEB J. 13 (1999) S23, (Suppl.).
[15] J.D. Feramisco, J.L. Goldstein, M.S. Brown, J. Biol. Chem. 279 (9) (2004) 8487.
[16] I. Walther, P. Pippia, M.A. Meloni, F. Turrini, F. Mannu, A. Cogoli, FEBS Lett. 436 (1) (1998) 115.
[17] K.B. Seamon, J.W. Daly, Adv. Cycl. Nucleotide Protein Phosphoryl. Res. 20 (1986) 1.
[18] T. van Daalen Wetters, P. Coffino, Methods Enzymol. 151 (1987) 9.
[19] J. Hochman, P.A. Insel, H.R. Bourne, P. Coffino, G.M. Tomkins, Proc. Natl. Acad. Sci. U. S. A. 72 (12) (1975) 5051.
[20] G.C. Ulett, N. Ketheesan, R.G. Hirst, Infect. Immun. 68 (4) (2000) 2034.
[21] D.R. DeSilva, E.A. Jones, M.F. Favata, B.D. Jaffee, R.L. Magolda, J.M. Trzaskos, P.A. Scherle, J. Immunol. 160 (9) (1998) 4175.
[22] N. Kanda, S. Watanabe, Biochem. Pharmacol. 62 (4) (2001) 495.
[23] A. Kvanta, M. Jondal, B.B. Fredholm, Biochim. Biophys. Acta 1093 (2–3) (1991) 178.
[24] J.A. Ledbetter, M. Parsons, P.J. Martin, J.A. Hansen, P.S. Rabinovitch, C.H. June, J. Immunol. 137 (10) (1986) 3299.
[25] G. Cohen, S. Rubinstein, Y. Gur, H. Breitbart, Dev. Biol. 267 (1) (2004) 230.
[26] S. Sugita, D.A. Baxter, J.H. Byrne, J. Neurosci. 17 (19) (1997) 7237.
[27] A.M. Michie, G. Rena, M.M. Harnett, M.D. Houslay, Cell Biochem. Biophys. 28 (2–3) (1998) 161.
[28] M. Liu, M.I. Simon, Nature 382 (6586) (1996) 83.
[29] A. Robinson-White, C.A. Stratakis, Ann. N.Y. Acad. Sci. 968 (2002) 256.
[30] N. Isakov, A. Altman, Annu. Rev. Immunol. 20 (2002) 761.
[31] S. John, C.M. Robbins, W.J. Leonard, EMBO J. 15 (20) (1996) 5627.
[32] W.K. Meyer, P. Reichenbach, U. Schindler, E. Soldaini, M. Nabholz, J. Biol. Chem. 272 (50) (1997) 31821.
[33] A. Kvanta, C. Nordstedt, M. Jondal, B.B. Fredholm, Naunyn-Schmiedeberg's Arch. Pharmacol. 340 (6 Pt 2) (1989) 715.
[34] A. Kvanta, P. Gerwins, M. Jondal, B.B. Fredholm, Cell. Signal. 2 (5) (1990) 461.
[35] P.J. Stork, J.M. Schmitt, Trends Cell Biol. 12 (6) (2002) 258.
[36] C. Ramstad, V. Sundvold, H.K. Johansen, T. Lea, Cell. Signal. 12 (8) (2000) 557.
[37] S. Sugita, D.A. Baxter, J.H. Byrne, J. Neurosci. 17 (1997) 7237.
[38] I.M. Adcock, G. Caramori, Immunol. Cell Biol. 79 (4) (2001) 376.
[39] R.C. Li, P. Ping, J. Zhang, W.B. Wead, X. Cao, J. Gao, Y. Zheng, S. Huang, J. Han, R. Bolli, Am. J. Physiol., Heart Circ. Physiol. 279 (4) (2000) H1679.
[40] L.W. Lo, J.J. Cheng, J.J. Chiu, B.S. Wung, Y.C. Liu, D.L. Wang, J. Cell. Physiol. 188 (3) (2001) 304.
[41] J.J. Cheng, B.S. Wung, Y.J. Chao, D.L. Wang, J. Biol. Chem. 276 (33) (2001) 31368.
[42] A.J. Shaywitz, M.E. Greenberg, Annu. Rev. Biochem. 68 (1999) 821.
[43] T.R. Sharif, M. Sharif, Int. J. Oncol. 14 (2) (1999) 327.
[44] K.K. Yamamoto, G.A. Gonzalez, W.H. Biggs III, M.R. Montminy, Nature 334 (6182) (1988) 494.
[45] P. Fields, F. Fitch, T. Gajewski, J. Mol. Med. 74 (11) (1996) 673.